2581-4575

International Journal For Recent Developments in Science & Technology

Crossref

A Peer Reviewed Research Journal

A SIMPLE ACTIVE AND REACTIVE POWER CONTROL FOR APPLICATIONS OF SINGLE-PHASE ELECTRIC SPRINGS

[#1]B.SWATHI, [#2]P.MANJUSHA

[1]M.TECH STUDENT, DEPARTMENT OF EEE, KAKINADA INSTITUTE OF TECHNOLOGICAL SCIENCES (KITS), RAMACHANDRAPURAM

[2]ASSISTANT PROFESSOR, DEPARTMENT OF EEE, KAKINADA INSTITUTE OF TECHNOLOGICAL SCIENCES (KITS), RAMACHANDRAPURAM.

Abstract —Aiming at effective power management in micro grids with high penetration of renewable energy sources (RESs), this paper proposes a simple power control for the so-called second-generation, single-phase electric springs (ES-2), which overcomes the shortcomings of the existing ES control methods. By the proposed control, the unpredictable power generated from RESs is divided into two parts, i.e., the one absorbed by the ES-2 that still varies and the other injected into the grid that is controllable by a simple and accurate signal manipulation that works both at steady-state and during RES transients. It is believed that such a control is suitable for the distributed power generation, especially at domestic homes. In this paper, the proposed control is supported by a theoretical background. Its effectiveness is at first validated by simulations and then by experiments. To this purpose, a typical RES application is considered, and an experimental setup is arranged, built up around an ES-2 implementing the proposed control. Testing of the setup is carried out in three steps and proves not only the smooth operation of the ES-2 itself, but also its capability in running the application properly.

Index Terms:- Distributed generation, electric spring (ES), grid connected, micro grids, power control, smart load (SL).

1. INTRODUCTION

Centralized control is adopted in the existing power system where power generation mainly depends on the load prediction. Nowadays, with the increasing portion of power generated from the renewable energy sources (RESs) and injected into the power system, stability issues become more and more severe due to the RES intermittency [1]. Flexible alternating current transmission systems are used to control voltage and/or power flow [2]–[5]. However, most of them are suitable for high- or medium-voltage applications, and cannot be used for future low-voltage micro grids with high RES penetration, such as roof photovoltaic and small power-rating wind plants [6]. To cope with this need, the electric spring (ES) technology has been proposed for future distributed micro grids [7] to transfer the line voltage fluctuations to the so-called noncritical loads (NCLs) [8], i.e., to the loads that tolerate a large supply voltage range, so as to keep regulated the voltage across the so-called critical loads (CLs), i.e., the loads that tolerate a narrow supply voltage range. The transfer occurs through an automatic balance of the load demand with the power generation, performed by ES. The set made of ES and NCLs forms the so-called smart load (SL). The voltage across CLs and the in-parallel SL is hereafter designated with CL voltage. So far, many papers have appeared reporting on ES topologies [8]–[11] and their control strategies [12]–[16]. The first version (ES-1) in [8] can only manage the reactive power whilst the second version (ES-2) in [9] can manage both the active and the reactive power as the capacitor in the dc

International Journal For Recent Developments in Science & Technology
2581-4575
Crossref
A Peer Reviewed Research Journal

side of ES is replaced with a voltage source like a battery pack. The third version (ES-3) in [10] is a new type of ES without NCL. The so sequenced fourth version (ES-4) in [11] changes the performance of ES greatly, since it compels the NCL voltage to vary in the same manner as the line voltage by the help of the insertion of an additional transformer in the original ES-2. Previous works have reported various control schemes of the ES-2 [13]–[15]. For instance, Yan et al. [13] propose the control of the input current by resorting to the dq0-transformation. This solution, however, is unable to keep unaltered the grid voltage as it is regulated in an open-loop mode. Even if a closed loop with a proportional integral (PI) regulator is added to regulate the grid voltage, it mainly takes care of the power factor correction rather than of the voltage regulation. In [14], the δ control is proposed to adjust the instantaneous phase of CL voltage but relies on system modeling that utilizes the circuitry parameters. Recently, the radial-chordal decomposition (RCD) control is proposed in [15] to decouple the control of the power angle of SL from the voltage across CL, which makes ES-2 ready to be embedded in many devices such as water heaters. However, it still has some shortcomings. For instance, the power angle of NCL should be known in advance, which prevents the use of the RCD control when NCL varies or is nonlinear. Besides, it is difficult to obtain pure reactive power compensation by means of ES. Wind power plant as an example the maximum power point tracking (MPPT) technique is normally adopted in the wind and/or solar power generation plants [17], [18]. The tracked active power is consumed by the electrical loads at domestic homes, which are of both CL and NCL types. For an ES installed at the same location as the wind power plant, the active and reactive powers generated by the plant can be measured by ES even if they are changing quickly. As a result, ES in such situations can carry out the control of both the input active and reactive power and, by the latter control, can regulate the rms value of the CL voltage at the preset value. For instance, the control scheme in [13] cannot handle the active power independently of the reactive one. Although constant active power compensation can be achieved by the δ control in [14], its shortcomings cannot still be overcome. Instead, the RCD control in [15] can regulate the grid voltage and can also correct the power factor of SL by the independent radial and chordal actions. However, Mok et al. [15] does not discuss the situation in which the input active power is constant. Even if one can demonstrate that the RCD control can deal with such a situation, calculations necessary to determine the reactive power that ES must provide are very involved, especially during the transients.

Aiming at the massive applications of ES-2 in the distributed power systems, this paper proposes a simple active and reactive power control as a solution to the shortcomings of the existing control methods. The proposed control not only decouples the active and reactive powers, but also relies on a local signal manipulation that does not need any information on the ES-2 circuitry parameters and the line voltage and parameters. Besides simulations, experiments are accomplished in three steps to verify the power management capabilities of the ES-2 implementing the proposed control.

In detail, this paper is organized as follows. Section II reviews the working principle of the ES-2 operated with the existing power control. Section III introduces the proposed power control and explains how it works. Section IV presents the simulations carried out on an ES-2 operated with the proposed control and discusses the simulation results. Section V gives experimental results obtained from a setup that consists of an ES-2 implementing the proposed control and a typical

International Journal For Recent Developments in Science & Technology
2581-4575
Crossref
A Peer Reviewed Research Journal

RES application. Finally, Section VI concludes the paper.

II. OPERATING PRINCIPLES OF ES-2

ES-2 Topology

As explained in [8], electric loads are divided into two types, namely CLs and NCLs. ES is an electrical device that is able to regulate the CL voltage at a preset value while passing the voltage (and power) fluctuations from the sources to NCL. The topology of ES-2 and the associated circuitry are drawn in Fig. 1. In this figure, ES-2 is enclosed by the dashed line and consists of a single-phase voltage source inverter (VSI), an L filter, and a capacitor whose voltage sums up to that of the NCL. Moreover, Z2 is the CL, Z3 is the NCL, vG represents the line voltage of the power system with RESs, R1 and L1 are the line resistance and inductance, respectively. The branch including vG and the line impedance supplies CL and SL. vS denotes the voltage of point of common coupling (PCC), which is also the CL voltage.

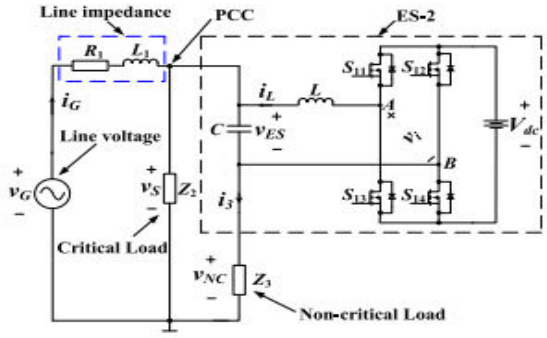

Fig. 1. Topology of ES-2 and associated circuitry.

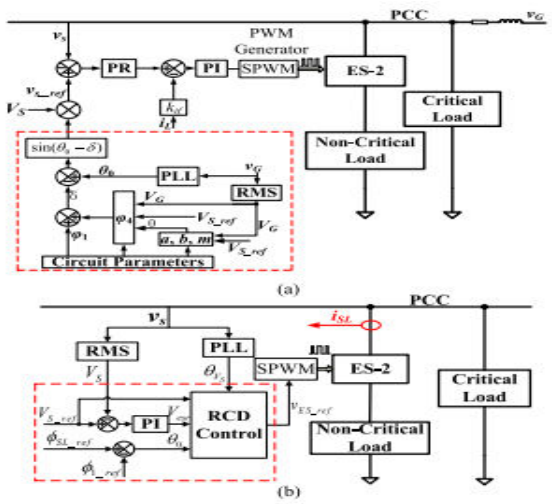

Fig. 2. ES-2 control diagrams for (a) δ control and (b) RCD control.

B. Power Control of Existing ES-2

δ control is one of the power control methods for ES-2; its diagram is shown in Fig. 2(a) and includes a double-loop control. The outer loop is closed around the CL voltage by means of a proportional resonant (PR) regulator whilst the inner one is closed around the ES current by means of a P regulator. The purpose of δ control is to set the instantaneous phase of the reference voltage for the PR regulator. The process of δ calculation is based on a vector analysis and ensures that ES operates at constant input active power mode [14]. Once the CL voltage is regulated, the control objectives of ES-2 are achieved. The δ calculation, which is executed by the blocks enclosed by the dashed line of Fig. 2(a), is the key element that affects operation of ES-2 and, hence, the fulfillment of the control objectives directly. However, δ calculation is based on a model of the ES-2 topology, shown in Fig. 1, and utilizes the parameters of the circuitry, thus, impairing the control accuracy as they vary. What's more, as δ control is a phase control based on a vector diagram, it requires the rms value of vG (marked as VG) to calculate the angle δ. Consequently, VG should be known in advance. In order to detect VG , communication technique is needed between two neighboring ESs because vG is far away from ES-2 due to the transmission line between the ES-2 and the grid. This drawback leads to cost up when applying δ control to ES-2.

The RCD control diagram for ES-2 is drawn in Fig. 2(b). The ES voltage is here decomposed into two directions, named the radial and chordal ones. The PCC voltage is regulated by adjusting the apparent power absorbed by SL using the radial control whilst the power angle of SL is regulated at the preset value by the chordal control. This feature makes the SL smart as it allows ES-2 to achieve independent control of the apparent power

International Journal For Recent Developments in Science & Technology
2581-4575
Crossref
A Peer Reviewed Research Journal

and the power angle of SL. From this perspective, it follows that the RCD control aims at the power control of SL.

Although it is not like the δ control that needs almost all the circuitry parameters, impedance angle of NCL must be known in advance. It is also very difficult to operate ES-2 at pure reactive power compensation mode. Besides, how to deal with the situation when input active power is varying is not explained in [15].

C. Requirements for the Proposed Power Control

Further to the analysis above, it would be desirable to dispose of a new power control method with the following requirements.

1) No need to detect the information of the grid voltage which is far away from PCC, like δ control

2) Need to decouple the control loop of the input active power from that of the PCC voltage or of the input reactive power

3) Easy to implement and less computational burden compared to other techniques

III. CONTROL OF ELECTRIC SPRINGS

Fig.4 shows a complete control block diagram of an electric spring. It consists of two closed loop controller including an AC voltage controller to regulate the power line voltage and a DC bus voltage controller to regulate the inverter dc bus voltage. The individual transfer function of the digital PI controller in discrete from is expressed as

$$u(t) = u(t-1) + K_P\left[e(t) - e(t-1)\right] + K_P \frac{T_S}{T_i} e(t) \qquad (1)$$

where u(t), u(t-1) and e(t), e(t-1) are the transfer function output and error input of the controller at the present and pass sampling, respectively. Kp is the proportional gain constant, Ti is the integral time constant and Ts is the sampling time of the controller.

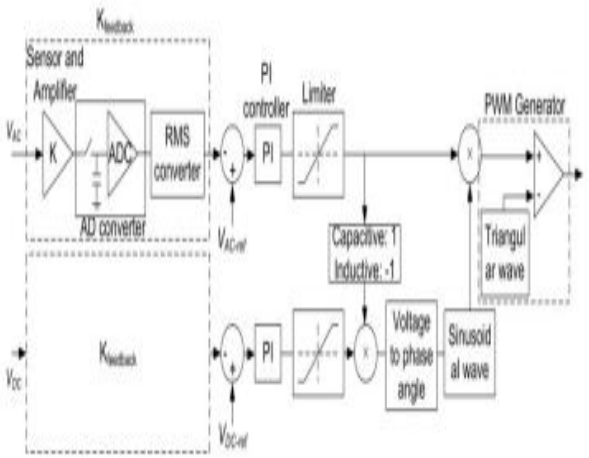

Fig. 4: Block diagram for electric spring control

The output of the PI compensator driving the AC line voltage error to zero decides the modulation index. The DC link voltage controller decides the phase angle of the injected voltage. When the angle of the reference sinusoidal voltage is measured with respect to the system current flowing through the non-critical voltage, it is going to be very close to 90 degrees. The deviation from 90 degree phase angle is decided by the real power exchange with the DC bus.

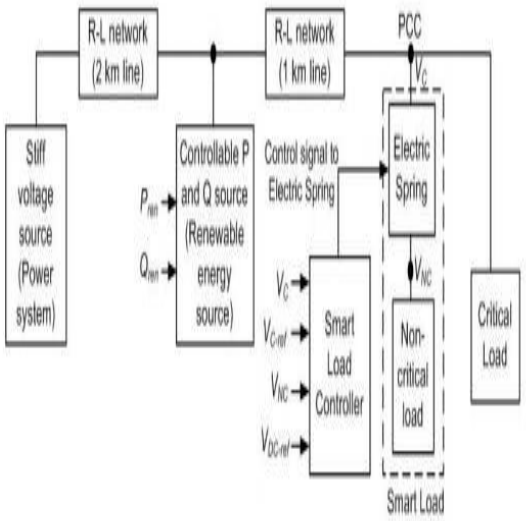

Fig. 5: Block diagram of the test system with Electric Spring

International Journal For Recent Developments in Science & Technology
2581-4575
Crossref
A Peer Reviewed Research Journal

IV.SIMULATIONS AND DISCUSSIONS

To verify the aforementioned analysis, simulations are conducted using MATLAB/Simulink based on parameters shown in Table I.

To simplify the analysis, both CL and NCL are chosen of resistive types. It should be noticed that they can be any other linear types. For the ES-2 system under simulation, the control objectives are formulated as follows: 1) rms value of the PCC

TABLE I
PARAMETERS FOR SIMULATION

Items	Values
Regulated PCC voltage (V_S)	220 V
DC bus voltage (V_{dc})	400 V
Line resistance (R_1)	0.1 Ω
Line inductance (L_1)	2.4 mH
CL (R_2)	43.5 Ω
NCL (R_3)	2.2 Ω
Inductance of low-pass filter (L)	3 mH
Capacitance of low-pass filter (C)	50 μF
Switching frequency (f_s)	20 kHz

voltage or input reactive power is regulated at preset values, and

2) input active power Pin tracks the preset value Pinref . Three situations are investigated, namely

1) Pinref varies at fixed VG ;

2) VG varies at fixed Pinref ;

3) Distorted VG .

A. Input Active Power Variation

In this part, three different values are selected for VG to monitor its behavior when Pinref varies. Fig. 5 shows the simulation results when Pinref varies. In each figure, four channels are recorded, reporting vG , Pinref , Pin , and rms value of the CL voltage, respectively.

Results in a full time range are also shown in Fig. 5(a), in which Pinref is changed from 1.6 to 1.1 kW at 0.4 s and then back to 1.6 kW at 0.8 s. It is observed that Pin tracks Pinref well while VS is regulated to 220 V as Pinref varies. To validate the proposed control further, the values of Pinref are raised and simulated, as shown in Fig. 5(b). The waveforms confirm that the control objectives are also realized at high power ratings.

To demonstrate how the control operates with the ES-2 power quantities, they are traced in Fig. 5(c), setting VG = 200 as an example. In each figure, four channels are recorded, reporting Pin , PCL, PES , and PNCL against their preset values. The four power quantities represent the input active power, and the active powers absorbed, respectively, by the CL, the ES-2, and the NCL. In the first channel of each figure, Pinref and Pin are traced with the dashed and solid lines, respectively. In Fig. 5(c), Pinref is set to 8 kW from 0 to 0.4 s, then to 4 kW from 0.4 to 0.8 s and then to 2 kW from 0.8 to 1.2 s. The results show that Pin takes its reference at steady state. The active power of CL is almost regulated to 1.1 kW during all the simulation time. When Pinref is set to 8 kW, the active powers of ES-2 and NCL are around 3.4 and 3.4 kW, respectively, which means that ES-2 is absorbing active power. However, when Pinref drops to 2 kW, the active powers of ES and NCL are around −420 W and 1.31 kW, which means that ES-2 is providing active power. The results also reveal that active powers of both ES and NCL vary in the same way as that of Pin . Therefore, ES not only acts as a power manager that passes the power fluctuations from input voltage sources to NCL, but also acts as an energy storage device that absorbs and/or provides powers.

International Journal For Recent Developments in Science & Technology
2581-4575
Crossref
A Peer Reviewed Research Journal

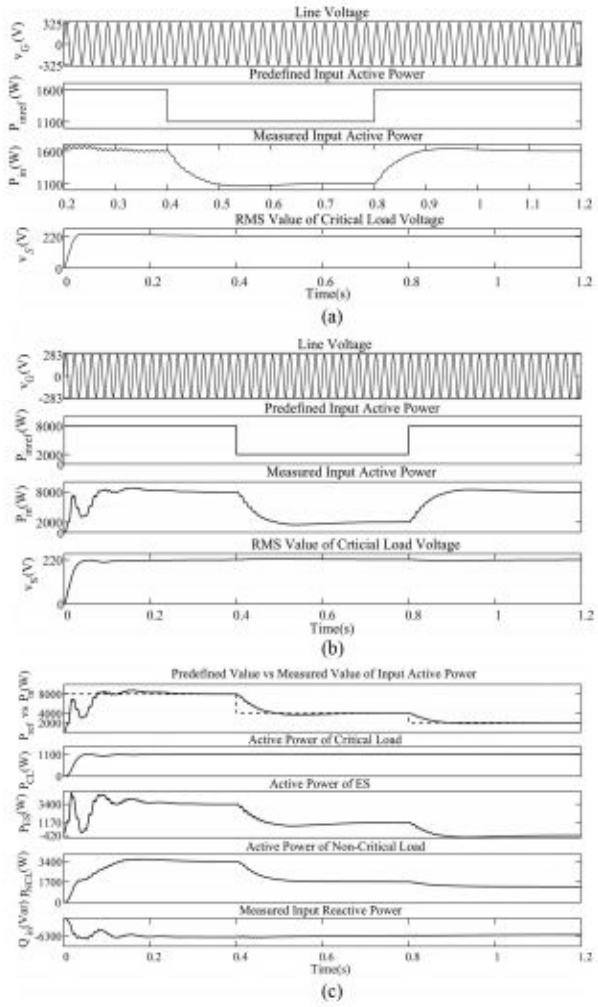

Fig. 5. Simulation waveforms under different variations of the input active power. (a) From 1.6 to 1.1 kW and then back to 1.6 kW at V_G = 230 V. (b) From 8 to 2 kW and then back to 8 kW at V_G = 200 V. (c) From 8 to 4 kW and then to 2 kW at V_G = 200 V.

B. Line Voltage Variation

In this section, the ES-2 transient responses to a change of VG are monitored with Pinref fixed. They are traced in Fig. 6(a) and (b). In each figure, four channels are recorded, reporting line voltage, reference value of the input active power, input active power, and rms value of CL voltage, respectively.

In Fig. 6(a), VG is changed between two different values, more specifically it is equal to 240 V from 0 to 0.5 s; afterward, it drops to 210 V at 0.5 s and remains at this value up to 1 s. The change of VG in Fig. 6(b) is the opposite of that in Fig. 6(a). In both the simulations, Pinref is set to 1.5 kW and Pin remains at the preset value very accurately. Meanwhile, the rms value of the CL voltage is regulated to 220 V as required.

C. Grid Distortion

In this part, performances of the ES system under grid distortion are observed. Besides, the waveforms of PLL are also provided, as shown in Fig. 7.

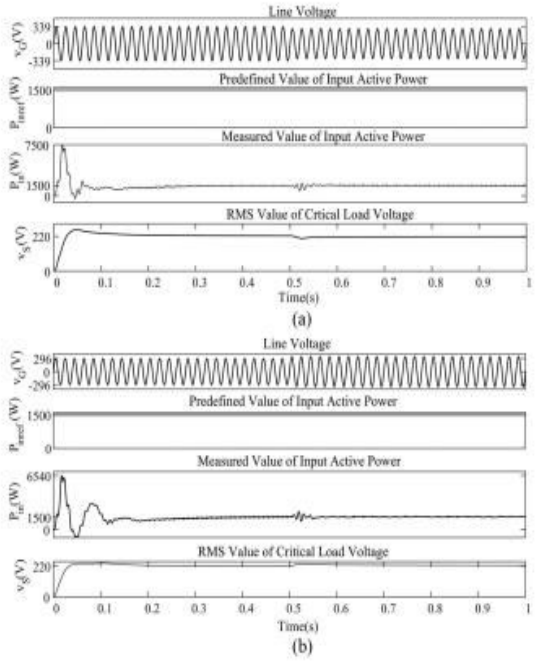

Fig. 6. Transient ES-2 responses to a change of the line voltage with P_{inref} = 1.5 kW. (a) From 240 to 210 V. (b) From 210 to 240 V.

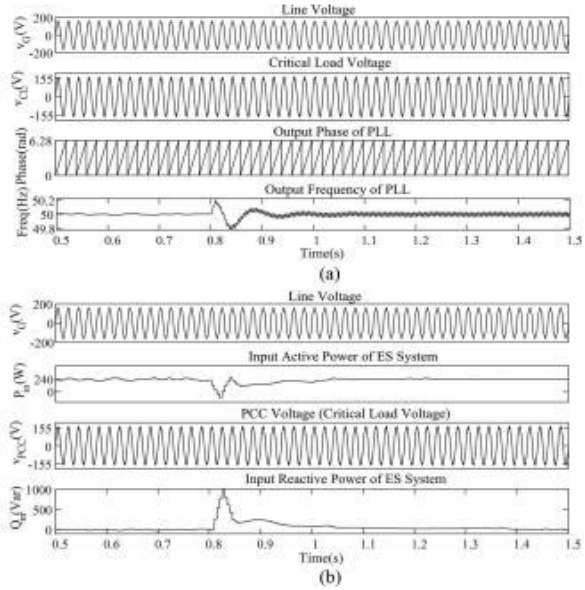

Fig. 7. Simulation waveforms before and after grid distortion. (a) Results of PLL. (b) Results of active and reactive power of ES system.

International Journal For Recent Developments in Science & Technology
2581-4575
Crossref
A Peer Reviewed Research Journal

In Fig. 7(a), four channels are recorded as line voltage, CL voltage which is also PCC voltage, output phase of PLL, and output frequency of PLL, respectively. From 0.5 to 0.8 s, VG is 110 V without any distortion. However, from 0.8 to 1.5 s, VG is added with the third and fifth harmonic components, each 11 V, respectively. It is seen that the output phase of PLL are stable during the simulation time even there is distortion on the line voltage. Before 0.8 s, the output frequency is stable at 50 Hz. Although fluctuations are seen in the output frequency in the fourth channel from 0.8 to 1.5 s, the fluctuating range is only from 49.97 to 50.03 Hz. Fig. 7(b)shows that the input active and reactive powers of ES system are also regulated well to follow the predefined values under the condition of grid distortion.

D. Discussions

The essence of a power control of the ES-2 can be summarized as follows. It can achieve only two objectives, namely 1) the regulation of the CL voltage by acting on the input reactive power, and 2) the control of the phase angle between voltage and current of the ES-2 by acting on the input active power.

Regarding δ control in [14], the key objective is the regulation of the CL voltage. All the compensation modes are related to the control of the phase angle between voltage and current of the ES-2. For instance, such phase angle should be precisely 90° at pure reactive power compensation mode. For the constant input active power control mode, the phase angle will no longer be 90°, but varies with the input active power. The same applies to the other compensation modes. From this point of view, the proposed control can cover all the cases of δ control by changing the upper loop in Fig. 3(a), not to mention that it gets rid of the circuitry parameters. The essence of the RCD control is to control both the CL voltage and the power angle of the SL. According to the analysis above, such control is encompassed by the proposed control if only just the upper loop in Fig. 3(a) is used to adjust the power angle of the SL.

To summarize, it emerges that, besides an easy implementation, the key advantage of the proposed control is that it works irrespectively of the circuitry parameters.

V. EXPERIMENTAL VALIDATION

A schematic overview of the experimental setup is shown in Fig. 9. It comprises of a 90 kVA inverter acting as a controlled power source. A separate 10 kVA inverter is used to emulate an intermittent renewable energy source capable of injecting variable active and/or reactive power which causes the voltage across the critical load to fluctuate. Both critical and non-critical loads are represented by resistors. Here the loads were considered to be resistive although they do not have to be necessarily resistive. The use of the ES for inductive and capacitive non-critical loads has been practically demonstrated in [14]. Distribution lines are represented by standard network boxes. The parameters used for the system and the electric spring (ES) are summarized ,respectively. Instantaneous voltage and current at different nodes of setup are recorded through a data acquisition system. A photograph of the experimental set up at the Maurice Hancock Smart Energy Laboratory at Imperial College London is shown in Fig. 10.

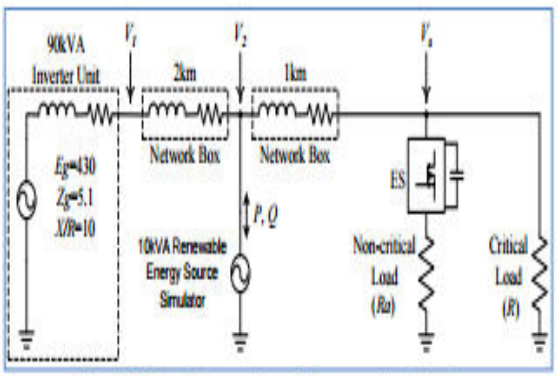

Fig. 9: Schematic overview of the experimental set up

International Journal For Recent Developments in Science & Technology
2581-4575
Crossref
A Peer Reviewed Research Journal

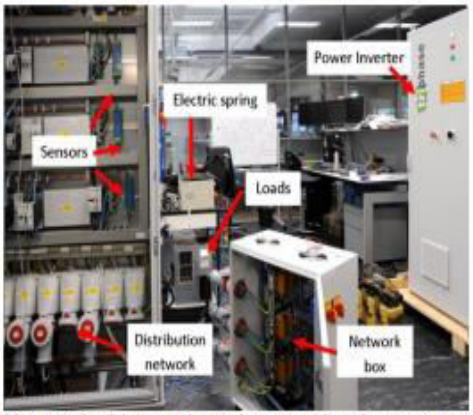

Fig. 10: Photograph of the experimental set up with major components shown

Three case studies were conducted to illustrate the operation of the ES and validate the model against experimental results. Firstly, the line voltage (i.e. voltage across the critical load) is decreased by increasing the reactive power consumption of the intermittent source and thereby, operating the ES in voltage support mode. Secondly, the line voltage is increased by decreasing the reactive power consumption of the intermittent source and thereby, operating the ES in voltage suppression mode. Finally, the reactive power absorption/injcetion by the intermittent source was varied randomly to test the voltage regulation capability of the ES and also validate its model by comparing the simulated response against the experiments.

In four channels are recorded as line voltage, CL voltage which is also PCC voltage, output phase of PLL, and output frequency of PLL, respectively. From 0.5 to 0.8 s, VG is 110 V without any distortion. However, from 0.8 to 1.5 s, VG is added with the third and fifth harmonic components, each 11 V, respectively. It is seen that the output phase of PLL are stableS1 and S2 . The second step is intended to check the behavior of the GCC in emulating the power injection from an RES and is performed by switching ON both S1 and S2 . The third step is intended to jointly debug both the ES-2 and the GCC to validate the effectiveness of the power control in a real application and is performed by switching S1 OFF and S2 ON.

A .Only the ES-2 is Activated (Step 1)

In this section, both S1 and S2 are turned OFF, which means that the ES-2 is activated and the GCC is detached. Theexperimental waveforms obtained from the ES-2 system are shown in Fig. 9(a) and (b), where three channels are recorded, reporting Pinref versus Pin , the CL voltage vS which is also PCC voltage, and the input reactive power Qin . As mentioned previously, Pin is the total active power absorbed by the CL, the NCL, and the ES-2. In Fig. 9(a), Qinref is set to 0 whilst Pinref is set to 240 W from 0 to 0.85 s and to 200 W from 0.85 to 1.5 s. It can be observed that Pin and Qin track the references smoothly. In Fig. 9(b), Pinref is set to 240 W whilst Qinref is set to 0 before 0.75 s and to 50 Var from 0.75 to 1.5 s. Before 0.75 s, the mean value of Pin is almost steady at 240 W, ignoring the moderate fluctuations. After 0.75 s, although decreasing a little just after the change of Qinref , Pin goes back to 240 W finally. Moreover, the third channel of Fig. 9(b) shows that Qin settles at the required value of 50 Var at steady state. Fig. 9(a) and (b) confirms the deocupled power control ability of ES-2 with the proposed control. In order to increase the readability, simulation results are added in Fig. 9(c) and (d), which are shown to compare with Fig. 9(a) and (b), respectively**.**

B. Only the GCC is Activated (Step 2)

In this section, both S1 and S2 are turned ON to deactivate the ES and connect the GCC. The purpose is to check the behavior of the PCC voltage with different power injections. In order to distinguish the power in different steps, the active and reactive power generated by the GCC are hereafter denoted with Pinj and Qinj, and the reference of Pinj is denoted with Pinjref . Besides, the current injected into PCC is termed as I0 . The active and reactive power control is also used in the GCC. The experimental waveforms are shown

International Journal For Recent Developments in Science & Technology
2581-4575
Crossref
A Peer Reviewed Research Journal

in Fig. 10, where the quantities in the first three channels are the same as in Fig. 9. The only difference is an additional channel to monitor I0 and the trace of PCC voltage is zoomed out by one-fifth of its normal value. In Fig. 10,

the reference value of Qinj is set to zero, which means that only active power is injected into PCC. The results point out that the control of Pinj works well as it keeps Pinj tracking Pinjref . Meanwhile, the current injected into PCC is controlled so as to be in phase with the PCC voltage also in the presence of a step variation of Pinj.

The reason why PCC voltage looks so stable with power injection is as follows. The intention of this part is to use GCC to simulate an intermittent power generated from RESs, which should be managed by the ES-2. In the distributed power system, a single power injection at one place has little influence due to its limited power rating. However, if many of such power generations inject power into the grid, the influence will be huge. The huge power injection into the grid could not be simulated in the laboratory due to limitation. As a result, such little active power injected by the GCC is so limited and has almost no influence on the PCC.

C. Joint Debug of the ES-2 and the GCC (Step 3)

In this section, only S2 is switched ON so that both the ES-2 and the GCC are activated and the power control ability of the ES-2 in a real application is tested. There are many situations of power change; three of them, which take place typically in practice, are presented here. The relevant experimental waveforms are shown in Fig. 11(a)–(d).

The measured quantities reported in the three channels of Fig. 11(a)–(c) are active power generated by GCC, active power absorbed by the ES system, and active power sent to the grid. In detail, Pinjref and Pinj are given in the first channel whilst Pinref and Pin are given in the second channel. The power sent to the grid is Pgrid which is given in the third channel.

In each situation, there is a step of the reference of active power. In Fig. 11(a), Pinjref and Pinref are set initially to 50 and 150 W, respectively, and then both are set to 100 W.

The results outline that both Pinj and Pin track their references, although the response time of Pin is more sluggish than that of Pinj. Initially, the GCC generates 50 W whilst the CL, the NCL, and the ES-2 absorb 150 W; hence the grid has to generate 100 W to meet the load demand. After the change of the power references, the active power generated by the GCC is almost completely absorbed by the ES-2 system. Consequently, the grid does not absorb nor provide any active power.

In Fig. 11(b), initially the GCC generates 150 W whilst the ES-2 system absorbs 50 W, the rest power being sent to the grid. The responses after the change of the power references are similar to those in Fig. 11(a). In Fig. 11(c), Pinjref and Pinref are set to be equal both before and after the change. It appears from the traces that the grid does not absorb nor provide any active power at steady state since Pinj and Pin remain nearly equal also after the power change. It can be deduced from the experimental results that, if the ES-2 and the GCC are located together, Pinj is properly detected and managed by the ES-2 so that the power sent to the grid that is controllable.

Fig. 11(d) is added to show the waveforms of the active power of ES-2, ES-2 voltage, and PCC voltage when the input active power is changing. It is seen that when Pinref changes from 150 to 100 W, the PCC voltage and Pin are controlled well. Meanwhile, the test result in channel 2 shows that the active power of ES also changes as Pin changes. After 1 s, when the input active power is low, the ES has to provide active power to make sure a stable power on the CL.

D. Remarks of Parameter Tuning

International Journal For Recent Developments in Science & Technology
2581-4575
Crossref
A Peer Reviewed Research Journal

It should be noted that the trial-and-error method was adopted during parameter tuning. The estimated controller bandwidth is about 40 Hz. The kp and ki of both PI controllers in Fig. 3(a) are set to 0.0008 and 0.02, respectively.

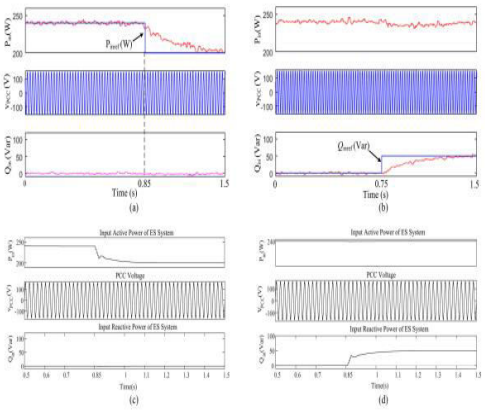

Fig. 9. Experimental and simulation results of the ES-2 system. (a) Experimental results of P_{inref} changing from 240 to 200 W whilst Q_{inref} is set to 0. (b) Experimental results of Q_{inref} changing from 0 to 50 Var whilst P_{inref} is set to 240 W. (c) Simulation results of P_{inref} changing from 240 to 200 W whilst Q_{inref} is set to 0. (d) Simulation results of Q_{inref} changing from 0 to 50 Var whilst P_{inref} is set to 240 W.

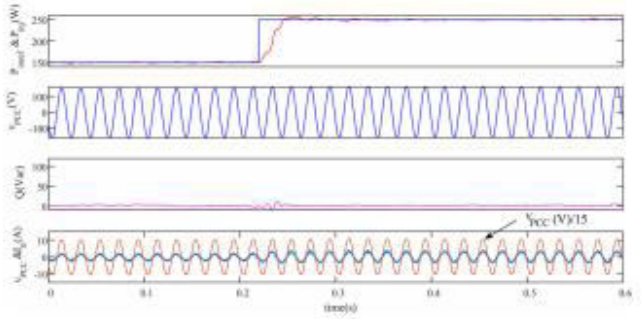

Fig. 10. Experimental waveforms when P_{injref} steps from 150 to 250 W whilst Q_{injref} is set to 0.

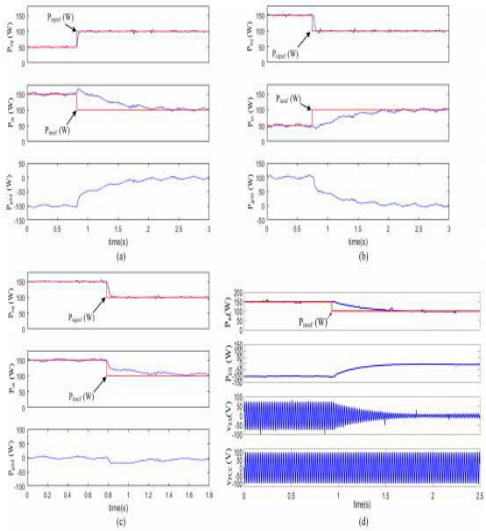

Fig. 11. Experimental waveforms at joint debugging of the ES-2 and the GCC under the simultaneous change of the active power references. (a) P_{injref} changes from 50 to 100 W and P_{inref} changes from 150 to 100 W. (b) P_{injref} changes from 150 to 100 W and P_{inref} changes from 50 to 100 W. (c) Both P_{injref} and P_{inref} change from 150 to 100 W. (d) Waveforms of active power of ES-2 and voltages of ES and PCC when P_{inref} changes from 150 to 100 W.

VI. CONCLUSION

The electric spring is a new technology that has attractive features including dynamic voltage regulation, balancing power supply and demand [8,9], power quality improvement [14], distributed power compensation [15] and reducing energy storage requreiments for future smart grid [16]. In order to fully explore their full potentials in large-scale power system simulation, an averaged simulation model for the electric spring is proposed here for the smart grid research community. The simulation model is simple for inclusion into large-scale system simulation platforms and yet accurate enough to capture the dynamic behavior of interest in terms of studying voltage and frequency stability. The case studies reported in the previous section exhibited close match between simulation and experimental results confirming the accuracy. The discrepancies, wherever applicable have been accounted for. These are due to the fact that the DC link voltage control loop has been neglected. This results in attaining a different operation point in terms of ES voltage inorder to obtain the same line voltage which is possible as suggested by the phasor diagrams in Fig. 3. It is possible, of course, to include the DC link voltage control loop in the model to eliminate these little discrepancies but only at the expense of significant increase in simulation time for large systems. The addition of DC link voltage control loop (with large number of ES distributed across the system) makes the simulation much more complex with little improvement in terms of accuracy. The use of 'Electric Springs' is a novel way of distributed voltage control while simultaneously achieving effective demand-side management through modulation of non-critical loads in response to the fluctuations in intermittent renewable energy sources (e.g. wind). This paper describes the simulation approach for electric springs which is appropriate for voltage and frequency control

International Journal For Recent Developments in Science & Technology
2581-4575
Crossref
A Peer Reviewed Research Journal

studies at the power system level. Close similarity between the simulation and experimental results gave us the confidence to use this electric spring model for investigating the effectiveness of their collective operation when distributed in large number across a power system. The proposed dynamic model is generic enough to study the performance of ESs under different load power factors and proportion of critical and non-critical loads. The effectiveness of an ES improves with the proportion of non-critical load.

REFERENCES

[1] M. Cheng and Y. Zhu, "The state of the art of wind energy conversion systems and technologies: A review," Energy Convers. Manage., vol. 88, pp. 332–347, Dec. 2014.

[2] P. Sotoodeh and R. D. Miller, "Design and implementation of an 11-level inverter with FACTS capability for distributed energy systems," IEEE J. Emerg. Sel. Topics Power Electron., vol. 2, no. 1, pp. 87–96, Mar. 2014.

[3] L. Wang and D. N. Truong, "Stability enhancement of a power system with a PMSG-based and a DFIG-based offshore wind farm using a SVC with an adaptive-network-based fuzzy inference system," IEEE Trans. Ind. Electron., vol. 60, no. 7, pp. 2799–2807, Jul. 2013.

[4] Y. Zhang, X. Wu, and X. Yuan, "A simplified branch and bound approach for model predictive control of multilevel cascaded H-bridge STATCOM," IEEE Trans. Ind. Electron., vol. 64, no. 10, pp. 7634–7644, Oct. 2017.

[5] W. Wang, L. Yan, X. Zeng, B. Fan, and J. M. Guerrero, "Principle and design of a single-phase inverter based grounding system for neutral-toground voltage compensation in distribution networks," IEEE Trans. Ind. Electron., vol. 64, no. 2, pp. 1204–1213, Feb. 2017.

[6] Q. Sun, J. Zhou, J. M. Guerrero, and H. Zhang, "Hybrid three-phase/singlephase microgrid architecture with power management capabilities," IEEE Trans. Power Electron., vol. 30, no. 10, pp. 5964–5977, Oct. 2015.

[7] P. Palensky and D. Dietrich, "Demand Side Management: Demand Response, Intelligent Energy Systems, and Smart Loads," IEEE Transactions on Industrial Informatics, vol. 7, pp. 381-388, 2011.

[8] A. Brooks, E. Lu, D. Reicher, C. Spirakis, and B. Weihl, "Demand Dispatch," IEEE Power and Energy Magazine,, vol. 8, pp. 20-29, 2010.

[9] D. Westermann and A. John, "Demand Matching Wind Power Generation With Wide-Area Measurement and Demand-Side Management," IEEE Transactions on Energy Conversion, vol. 22, pp. 145-149, 2007.

[10] A. Mohsenian-Rad, "Autonomous Demand-Side Management Based on Game-Theoretic Energy Consumption Scheduling for the Future Smart Grid," IEEE Transactions on Smart Grid, vol. 1, pp. 320-331, 2010.

[11] S. C. Lee, "Demand Side Management With Air Conditioner Loads Based on the Queuing System Model," IEEE Transactions on Power Systems, vol. 26, pp. 661-668, 2011.

AUTHOR'S PROFILE:

[1]. B.SWATHI Pursuing her Masters Degree in Department of EEE from Kakinada Institute Of Technological Sciences (Kits), Ramachandrapuram.

[2]. POLINATI MANJUSHA, Completed her B.Tech and M.Tech Degrees from KITS Ramachandrapuram in EEE Department. Presently she is working as Assistant Professor in KITS Ramachandrapuram. Her Interested areas are Power Electronics.

2581-4575

International Journal For Recent Developments in Science & Technology

Crossref

A Peer Reviewed Research Journal